

# Cholesterol-rich Fluid Membranes Solubilize Ceramide Domains

## IMPLICATIONS FOR THE STRUCTURE AND DYNAMICS OF MAMMALIAN INTRACELLULAR AND PLASMA MEMBRANES<sup>\*[5]</sup>

Received for publication, February 10, 2009, and in revised form, May 28, 2009. Published, JBC Papers in Press, June 11, 2009, DOI 10.1074/jbc.M109.026567

Bruno M. Castro<sup>‡</sup>, Liana C. Silva<sup>‡</sup>, Alexander Fedorov<sup>‡</sup>, Rodrigo F. M. de Almeida<sup>§1</sup>, and Manuel Prieto<sup>‡2</sup>

From the <sup>‡</sup>Centro de Química-Física Molecular and Institute of Nanoscience and Nanotechnology, Instituto Superior Técnico, Complexo I, Avenida Rovisco Pais, 1049-001 Lisbon and the <sup>§</sup>Centro de Química e Bioquímica, Faculdade de Ciências da Universidade de Lisboa, Campo Grande, 1749-016 Lisbon, Portugal

A uniquely sensitive method for ceramide domain detection allowed us to study in detail cholesterol-ceramide interactions in lipid bilayers with low (physiological) ceramide concentrations, ranging from low or no cholesterol (a situation similar to intracellular membranes, such as endoplasmic reticulum) to high cholesterol (similar to mammalian plasma membrane). Diverse fluorescence spectroscopy and microscopy experiments were conducted showing that for low cholesterol amounts ceramide segregates into gel domains that disappear upon increasing cholesterol levels. This was observed in different raft (sphingomyelin/cholesterol-containing) and non-raft (sphingomyelin-absent) membranes, *i.e.* mimicking different types of cell membranes. Cholesterol-ceramide interactions have been described mainly as raft sphingomyelin-dependent. Here sphingomyelin independence is demonstrated. In addition, ceramide-rich domains re-appear when either cholesterol is converted by cholesterol oxidase to cholestenone or the temperature is decreased. Ceramide is more soluble in cholesterol-rich fluid membranes than in cholesterol-poor ones, thereby increasing the chemical potential of cholesterol. Ceramide solubility depends on the average gel-fluid transition temperature of the remaining membrane lipids. The inability of cholestenone-rich membranes to dissolve ceramide gel domains shows that the cholesterol ordering and packing properties are fundamental to the mixing process. We also show that the solubility of cholesterol in ceramide domains is low. The results are rationalized by a ternary phospholipid/ceramide/cholesterol phase diagram, providing the framework for the better understanding of biochemical phenomena modulated by cholesterol-ceramide interactions such as cholesterol oxidase activity, lipoprotein metabolism, and lipid targeting in cancer therapy. It also suggests that the lipid compositions of different organelles are such that ceramide gel domains are not formed unless a stress or pathological situation occurs.

Cholesterol (Chol)<sup>3</sup> is the most abundant sterol in mammalian plasma membrane and has unique biophysical properties (1, 2). Chol interacts with the high melting temperature ( $T_m$ ) sphingolipids (SL) in the membrane, leading to the formation of SL/Chol-enriched microdomains (so-called lipid rafts). These domains are in a more ordered state (usually referred to as liquid-ordered ( $l_o$ ) phase) than the bulk membrane (liquid-disordered phase ( $l_d$ )) (3, 4). Ceramide (Cer) is an SL formed in stress situations either from sphingomyelin (SM) in rafts or synthesized *de novo* by serine palmitoyltransferase and ceramide synthase. Both of these processes can be induced by diverse stimuli (5). Cer-induced membrane alterations (*e.g.* raft fusion into large signaling platforms (6)) were proposed to be the mechanism by which this lipid mediates diverse cellular processes, namely apoptosis (7–10). Cer presents an unusually small polar headgroup and in general very high gel-fluid  $T_m$  (*e.g.* for palmitoyl-Cer (PCer) it is  $\sim 90^\circ\text{C}$ ) (11). Membrane Cer levels are usually very low, although in cells undergoing apoptosis it can reach values up to 12 mol % total lipid (7), a percentage that in model membranes leads to Cer-rich gel domain formation (12–17). It was suggested that the formation of these domains might also be involved in Cer biological action (8, 18, 19).

However, Cer effects on membrane properties are extremely dependent on membrane lipid composition, especially on Chol amounts (13, 20–23). For instance, in raft-forming model membranes (*i.e.* ternary mixtures of phosphocholines (PC), sphingomyelin (SM), and Chol), Cer-rich gel domains are formed at low but not at high Chol content (23). This result was explained by the competition between the two small headgroup molecules, Chol and Cer, for the bulkier headgroup, SM, to minimize acyl chain exposure to water. In fact, it is suggested that Cer selectively displaces Chol molecules from rafts, both in model (24–27) and in cell membranes (28, 29). However, a recent study showed that Cer-generated from SM hydrolysis

\* This work was supported in part by Fundação para a Ciência e Tecnologia, Portugal, Research Grant POCTI/QUI/68151/2006 (to R. F. M. de A.), and Fellowships BD/36635/2007 (to B. M. C.) and BPD/30289/2006 (to L. C. S.).

[5] The on-line version of this article (available at <http://www.jbc.org>) contains supplemental Figs. S1–S4.

<sup>1</sup> To whom correspondence should be addressed: Centro de Química e Bioquímica, Faculdade de Ciências da Universidade de Lisboa, Campo Grande, Ed. C8, 1749-016 Lisboa, Portugal. Tel.: 351-217-500-924; Fax: 351-217-500-088; E-mail: rodrigo.almeida@fc.ul.pt.

<sup>2</sup> Recipient of support from Fundação para a Ciência e Tecnologia, Portugal.

<sup>3</sup> The abbreviations used are: Chol, cholesterol; Cer, ceramide; PCer, palmitoyl-Cer; POPC, 1-palmitoyl-2-oleoyl-*sn*-glycero-3-phosphocholine; DOPC, 1,2-dioleoyl-*sn*-glycero-3-phosphocholine; Chne, cholestenone; DPH, 1,6-diphenyl-1,3,5-hexatriene; *t*-PnA, *trans*-parinaric acid; Rho-DOPE, 1,2-dioleoyl-*sn*-glycero-3-phosphoethanolamine-*N*-lissamine rhodamine B sulfonyle;  $l_o$ , liquid-ordered phase;  $l_d$ , liquid-disordered phase; SL, sphingolipids; SM, sphingomyelin; PSM, palmitoyl-SM; PC, phosphocholine;  $T_m$ , main transition temperature; PM, plasma membrane; ER, endoplasmic reticulum; GUV, giant unilamellar vesicles.

leads to the formation of gel domains in these ternary mixtures only when Chol levels are low, suggesting that even for SM-depleted mixtures Chol is still able to modulate Cer effects (30). Therefore, to fully disclose the conditions that lead to the activation/regulation of Cer-mediated processes, further knowledge about Cer effects on membrane properties and their modulation by Chol is required.

It is important to clarify the relation between Cer threshold for gel formation, cholesterol amount, and the properties of the remaining lipids (namely their propensity to form gel phases, which depends mainly on their gel-fluid transition temperature). This is because of the fact that each organelle membrane has its own specific composition. For example, there is a gradient of cholesterol concentration from the endoplasmic reticulum (ER) to the plasma membrane (PM) (31). In addition, there is a close relation between intracellular Cer levels,  $\text{Ca}^{2+}$  release from the ER, and Cer-induced permeability increase of the mitochondrial outer membrane (but not the inner membrane) (32, 33).

The application of a uniquely sensitive method for Cer-rich gel detection allowed us to study for the first time Chol-Cer interactions in detail for high Chol and low Cer concentrations, *i.e.* a composition similar to mammalian plasma membranes. In addition, low Chol membranes were also studied. Our results clearly show that in a fluid matrix of representative mammalian membranes lipids, Cer-rich gel domains are destroyed by high amounts of Chol in the absence of SM and even in the absence of an  $l_o$  phase. We show that this outcome is a consequence of the higher solubility of Cer in Chol-rich membranes than in poor ones, the low solubility of Chol in Cer domains, and that it depends on the average  $T_m$  of the remaining lipids. These solubility differences offer a unified rationale for all Cer-Chol biophysical studies that can be translated into a ternary phase diagram, and the biological implications of the results are discussed.

## EXPERIMENTAL PROCEDURES

**Materials**—1-Palmitoyl-2-oleoyl-*sn*-glycero-3-phosphocholine (POPC), palmitoyl-SM (PSM), PCer, di-oleoyl-*sn*-glycero-3-phosphocholine (DOPC), and 1,2-dioleoyl-*sn*-glycero-3-phosphoethanolamine-*N*-lissamine rhodamine B sulfonyl (Rho-DOPE) were obtained from Avanti Polar Lipids (Alabaster, AL). Chol, recombinant Chol oxidase expressed in *Escherichia coli* (C1235), peroxidase from horseradish (P8250), and other chemicals for Chol oxidation measurements were from Sigma. 4-Cholesten-3-one (Chne) was obtained from Steraloids (Newport, RI). 1,6-Diphenyl-1,3,5-hexatriene (DPH) and *trans*-parinaric acid (*t*-PnA) were from Invitrogen. All organic solvents were UVASOL grade from Merck.

**Liposome Preparation**—Large unilamellar vesicles (0.2  $\mu\text{m}$ ) were obtained from multilamellar vesicles by the extrusion technique, as described previously (23). The suspension medium was 10 mM sodium phosphate, 150 mM NaCl, 0.1 mM EDTA buffer (pH 7.4). The probe/lipid ratios used were 1:200 for DPH and 1:500 for *t*-PnA. The concentration of lipids and probes in stock solutions was determined as described previously (17). GUVs labeled with Rho-DOPE (probe to lipid ratio

of 1:500) were prepared by electroformation, as described previously (34).

**Absorption and Fluorescence Measurements**—The absorption and steady-state measurements were conducted as described previously (35).

The fluorescence decay measurements were obtained by the single photon timing technique with laser pulse excitation, using  $\lambda_{\text{exc}}/\lambda_{\text{em}}$  295/405 nm for *t*-PnA (secondary laser of rhodamine 6G (34)). To obtain the fitting curves, the experimental decays were analyzed using the TRFA software (Scientific Software Technologies Center, Minsk, Belarus). The fluorescence decays are described ( $\chi^2 < 1.2$ ) by a sum of up to three exponentials (lifetime components) in the absence of gel phase. The presence of a Cer gel phase gives rise to an extra long component to achieve  $\chi^2 < 1.2$  and random distribution of weighted residuals. Without introducing another component in the analysis,  $\chi^2 > 1.6$  and the distribution of weighted residuals is nonrandom.

**Chol Oxidase-treated Membranes**—Large unilamellar vesicles (1 mM total lipid) were prepared as described above and incubated at 37 °C in 50 mM potassium phosphate buffer (pH 7.0) with or without Chol oxidase (1.5 units/ml). After Chol oxidation, the samples were diluted to 0.2 mM total lipid, and the probe was added.

**Confocal Fluorescence Microscopy**—Microscopy was performed in a Leica TCS SP5 (Leica Microsystems CMS GmbH, Mannheim, Germany) inverted microscope (DMI6000) with a 63 $\times$  water (1.2 numerical aperture) apochromatic objective as described previously (36). Quantification of gel domain fraction area was performed, using ImageJ software.

## RESULTS

**Chol in High Amounts Dissolves Cer-rich Gel Domains in Different Types of Fluid Membranes**—The interactions Chol-PCer were studied in a fluid matrix of POPC or DOPC by fluorescence spectroscopy and microscopy. Both are non-raft-forming mixtures because there was no observation of liquid-liquid immiscibility on the micron scale, for which the presence of sphingomyelin or another high  $T_m$  lipid such as a long chain saturated PC is necessary (37). However, although one leads to the formation of  $l_o$ -like heterogeneities at the temperatures used in this study (POPC/Chol), the other (DOPC/Chol) does so only for negative temperatures (38–40). Chol-PCer interactions were studied for physiological amounts of each lipid. In these conditions, the fraction of PCer-rich gel formed is low (15) and therefore extremely difficult to identify. The only method that is exceptionally sensitive to detect PCer-rich gel formation even at very low fractions is *t*-PnA fluorescence lifetime. The fluorescence properties of this membrane probe are very sensitive to the presence of gel phases (35), in particular to the PCer-rich gel. *t*-PnA has a high preference toward these gel domains where its fluorescence decay presents a fingerprinting component with a lifetime longer than 30 ns (15, 17, 23). These properties make *t*-PnA an exceptional probe for detecting PCer-rich gel domains, and thus the most suitable to investigate Chol-Cer interactions.

In ternary mixtures composed of POPC/Chol/PCer or DOPC/Chol/PCer, *t*-PnA fluorescence lifetimes show that

## Ceramide Solubilization in Cholesterol-rich Fluid Membranes

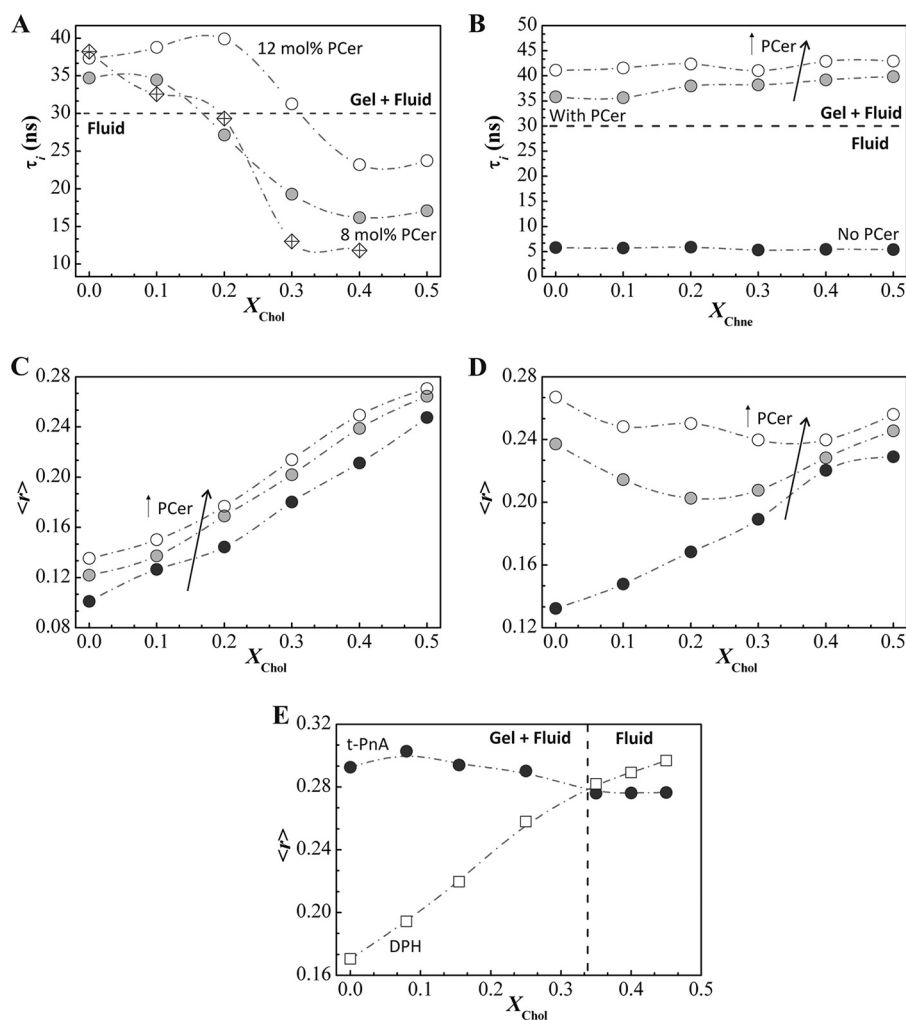


**FIGURE 1. Chol, but not Chne, dissolves Cer-rich gel domains.** Longest lifetime components of *t*-PnA fluorescence decay ( $\tau_1$ ) as a function of steroid mole fraction in POPC/Chol mixtures containing 8 (gray circles) and 12 mol % PCer (white circles) and DOPC/Chol mixtures containing 12 mol % PCer (crossed diamonds) (shown in A), and POPC/Chne mixtures containing 0 (black circles), 8 (gray circles), and 12 mol % PCer (white circles) at 24 °C (shown in B). Steady-state fluorescence anisotropy of DPH (C) and *t*-PnA (D) as a function of  $X_{\text{Chol}}$  in POPC/Chol mixtures containing 0 (black circles), 8 (gray circles), and 12 (white circles) mol % PCer at 24 °C, are shown. E, *t*-PnA (black circles) and DPH (white squares) steady-state anisotropy in POPC/Chol mixtures containing 20 mol % PCer. The dashed lines are merely to guide the eye.  $X_{\text{Chol}}$  and  $X_{\text{Chne}}$  are steroid mole fraction in the PC/steroid fraction of the membrane. All the values are the average of at least three independent measurements. The error bars are contained in the symbols.  $\langle r \rangle$ , steady-state fluorescence anisotropy.

PCer-rich gel domains are abolished by high amounts of Chol (Fig. 1A). For low mole fractions of Chol ( $X_{\text{Chol}}$ ), the lifetime of the long component of *t*-PnA fluorescence decay is above 30 ns, showing that PCer-rich gel domains are formed. Increasing  $X_{\text{Chol}}$ , the lifetime of this component decreases to values below 30 ns, showing that PCer-rich gel domains are no longer formed. This effect is independent of the phospholipid that constitutes the fluid matrix, because the same result is obtained for mixtures with either POPC or DOPC and therefore is independent of the phase formed in these mixtures at high Chol content, and there is no need for a  $l_o$  phase to be formed.

However, the amount of PCer necessary to form gel domains is different. Higher amounts of PCer are required to form gel in DOPC membranes (10 mol %; results not shown) as compared with POPC (4 mol %) (15). In addition, for the same amount of PCer (4 mol %), the Chol threshold for solubilization of a Cer gel is higher in the case of POPC (~40 mol %) than for DOPC

(~20 mol %) (Fig. 1A), *i.e.* Cer gel domains form more readily and solubilize with more difficulty in the membranes containing the phospholipid with higher  $T_m$ .

*t*-PnA and DPH steady-state fluorescence anisotropy ( $\langle r \rangle$ ) in POPC/Chol/PCer mixtures (Fig. 1, C–E) also report PCer-rich gel dissolution by Chol. The information retrieved from anisotropy measurements is complementary to that contained in fluorescence lifetimes (41). Whereas the lifetimes allow the detection and the identification of a particular phase, the anisotropy values only reflect the global order of the bilayer. In this way, other probes can be used to identify changes undergone in lipid domain organization when a dynamic change occurs, such as a temperature change or Chol oxidation (see below). This allows us to plan experiments that do not rely solely on *t*-PnA fluorescence but also in the fluorescence of other probes (*e.g.* DPH), thus providing further support to the results described above. However, to do so, it is necessary to measure the anisotropy values of the probes as a function of membrane composition. This was done, and the results are shown in Fig. 1, C–E. In the absence of PCer and Chol, DPH and *t*-PnA fluorescence anisotropy values are low and typical of a fluid (disordered) phase, presenting a linear increase with  $X_{\text{Chol}}$  due to the ordering effect of Chol in POPC acyl chains (42). In the presence of PCer, *t*-PnA fluorescence anisotropy presents a different profile. For low Chol amounts, *t*-PnA anisotropy values are high and typical of a gel-fluid coexistence (15, 17), showing that the membrane has a global order similar to that of a liquid-ordered phase. Increasing Chol content, the variations are unpronounced because as the gel phase melts, liquid-ordered phase is formed, and global order of the bilayer remains practically unchanged. The difference between *t*-PnA anisotropy values in mixtures containing PCer and the ones obtained in the absence of PCer is successively attenuated, until there is no difference. DPH is excluded from the highly compact PCer-rich gel (15, 17, 23), reporting only the order of the fluid phase. Therefore, its anisotropy is only slightly sensitive to PCer, presenting a small yet noticeable increase with  $X_{\text{PCer}}$  (Fig. 1C). As expected, by increasing Chol, DPH anisotropy increases, and at high Chol it presents values similar to the ones obtained for *t*-PnA (Fig. 1E). This result clearly shows that for high Chol

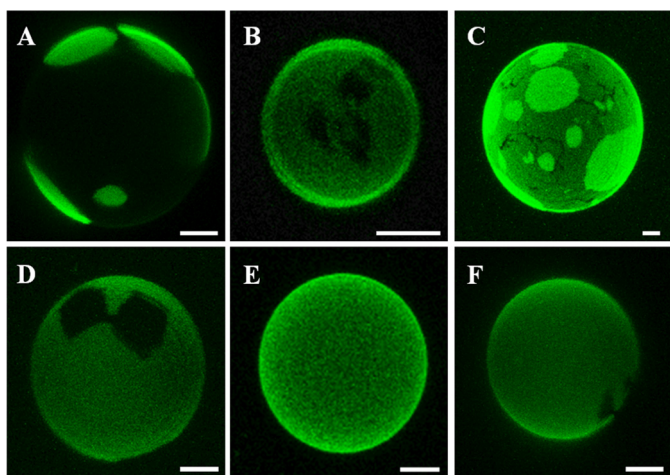


**FIGURE 2. Lipid domain formation as observed by confocal fluorescence microscopy.** Three-dimensional projection images obtained from confocal sections of GUV labeled with Rho-DOPE (0.2 mol %) at 24 °C are shown. GUVs were prepared from mixtures of PSM/POPC/Chol (1:1:1) (A) and PSM/POPC/Chol (13:30:7) (B) with 4 mol % PCer; PSM/POPC/Chol (1:1:1) (C) with 8 mol % PCer; POPC/Chol (9:1) (D) with 12 mol % PCer; POPC/Chol (3:2) (E) with 20 mol % PCer; and POPC/Chne (3:2) (F) with 12 mol % PCer, respectively. (Scale bar, 5  $\mu$ m).

content both probes report the same phase and that PCer-rich gel domains are not formed at high Chol. In addition, the trend of DPH anisotropy shows that the composition of the fluid is very similar in POPC/Chol content both in the absence and presence of different amounts of Cer, suggesting that the gel phase is mostly formed by Cer irrespective of the other components.

**Cer-rich Gel Dissolution by Chol Is Independent of Raft Formation (Presence of SM)**—As an alternative approach to study Chol-Cer interactions, we used GUV labeled with Rho-DOPE and confocal fluorescence microscopy (Fig. 2). Rho-DOPE presents an unfavorable partition to the  $l_o$  phase and a highly unfavorable partition to the gel phase (34). Thus, the  $l_d$  phase is seen as bright round regions,  $l_o$  as lesser bright than  $l_d$  round regions, and gel as non-round dark regions. For the typical raft mixture of POPC/palmitoyl-sphingomyelin (PSM)/Chol (1:1:1) with 4 mol % PCer mixtures, round shaped domains typical of an  $l_d/l_o$  phase separation are observed, and no gel domains are detected (Fig. 2A). For low Chol content, dark non-round gel regions are clearly observed both in the presence (Fig. 2B) and in the absence of SM (Fig. 2D). Conversely, for high Chol amounts, no gel is observed (Fig. 2, A and E). Dark non-round domains, *i.e.* PCer-rich gel domains, are observed at high Chol fraction in raft mixtures containing 8 mol % PCer (Fig. 2C) showing that there is a limit for the ability of Chol to dissolve those domains. Note that for POPC or DOPC mixtures with PCer and Chol, less than 33 mol %, Chol is enough to dissolve all the gel formed in the presence of 8 mol % Cer, once again indicating a correlation between the  $T_m$  of the phospholipid portion of the bilayer and the stability of Cer gel domains (PSM has a  $T_m$  of  $\sim 41$  °C (42), thus the average  $T_m$  values of the systems studied change in the order PSM/POPC > POPC > DOPC).

In SM-containing mixtures, Cer-rich gel dissolution by Chol was previously explained by the competition of these two molecules for the bulkier headgroup SM (27). However, in this study, Cer mixing in the fluid was also observed in the absence of SM, by both fluorescence spectroscopy (Fig. 1) and micros-

copy (Fig. 2) in different types of membrane model systems. Thus, Chol-induced Cer mixing cannot be explained by the competition between Chol and Cer for SM. Consequently, Cer-rich gel solubilization depends chiefly on the amount of Chol and next on the propensity of the remaining lipids to form a gel phase, as in the case of membranes containing PSM (a lipid with much higher  $T_m$  than DOPC or POPC), where the ability Cer to drive gel-fluid phase separation is higher (Figs. 2 and 3).

**Cholestenone Promotes Cer Demixing and Gel Phase Formation**—Cholestenone (Chne) is a steroid that is derived from Chol oxidation catalyzed by the enzyme Chol oxidase (EC 1.1.3.6). It has been reported that Chne cannot form ordered domains (43). To get further insights about the molecular mechanism leading to Cer-rich gel abolishment by Chol, we used Chne instead of Chol. This allows understanding if Cer gel dissolution is related to Chol special membrane ordering and packing properties or just to the presence of a bulky steroid ring structure. In the absence of PCer, and for all Chne fractions, the fluorescence intensity decay of *t*-PnA presents a component no longer than 6 ns. This confirms the inability of Chne to increase membrane order (Fig. 1B, bottom line).

Conversely, in PCer-containing mixtures, an extra long component with a value always >30 ns is necessary to describe properly (see “Experimental Procedures”) *t*-PnA fluorescence decay (Fig. 1B, top lines). This means that PCer-rich gel is present for all the  $X_{\text{Chne}}$  studied. *t*-PnA and DPH steady-state fluorescence anisotropy also support these results (supplemental Fig. S1). Further evidence for PCer-rich gel formation in the presence of Chne is obtained from confocal microscopy of GUV composed of POPC/Chne/PCer (Fig. 2F). Two distinct areas are clearly observed, a darker region that corresponds to the PCer-rich gel and a brighter region that corresponds to the POPC-rich fluid, which is the major phase. These results suggest that Cer solubilization by Chol is related to the special properties of Chol-rich membranes.

**Cer-rich Gel Domain Dissolution by Chol Is Reversible**—As mentioned, Cer-rich gel domain dissolution by Chol is independent of the presence of SM. Therefore, only two rationalizations are possible. One of the two following hypotheses explains what happens upon increasing the Chol content: 1) Cer is completely segregated and displaced from the membrane, because it becomes completely insoluble and incompatible with the bilayer structure (25); 2) Cer domains do not form because Cer is more soluble in Chol-rich membranes.

Regarding hypothesis 1, the formation of Cer crystals in a nonbilayer phase was observed by us in POPC/ceramide mixtures for very high ceramide content (15). In addition, others have observed (25) that the bilayer solubility limit of Chol and Cer was negatively affected by their mutual presence. Although in this study we used only small amounts of Cer and never reached the same total levels of Cer + Chol as those in Ali *et al.* (25), we considered hypothesis 1 because it explains most of the fluorescence data in equilibrium. If Cer is in fact excluded from the membrane by high amounts of Chol, this process is irreversible, because Cer in aqueous solution is not able to incorporate into the lipid bilayer (results shown in supplemental Fig. S2).

Regarding hypothesis 2, if Cer is solubilized in the membrane, then it should be possible to reform Cer gel, upon chang-

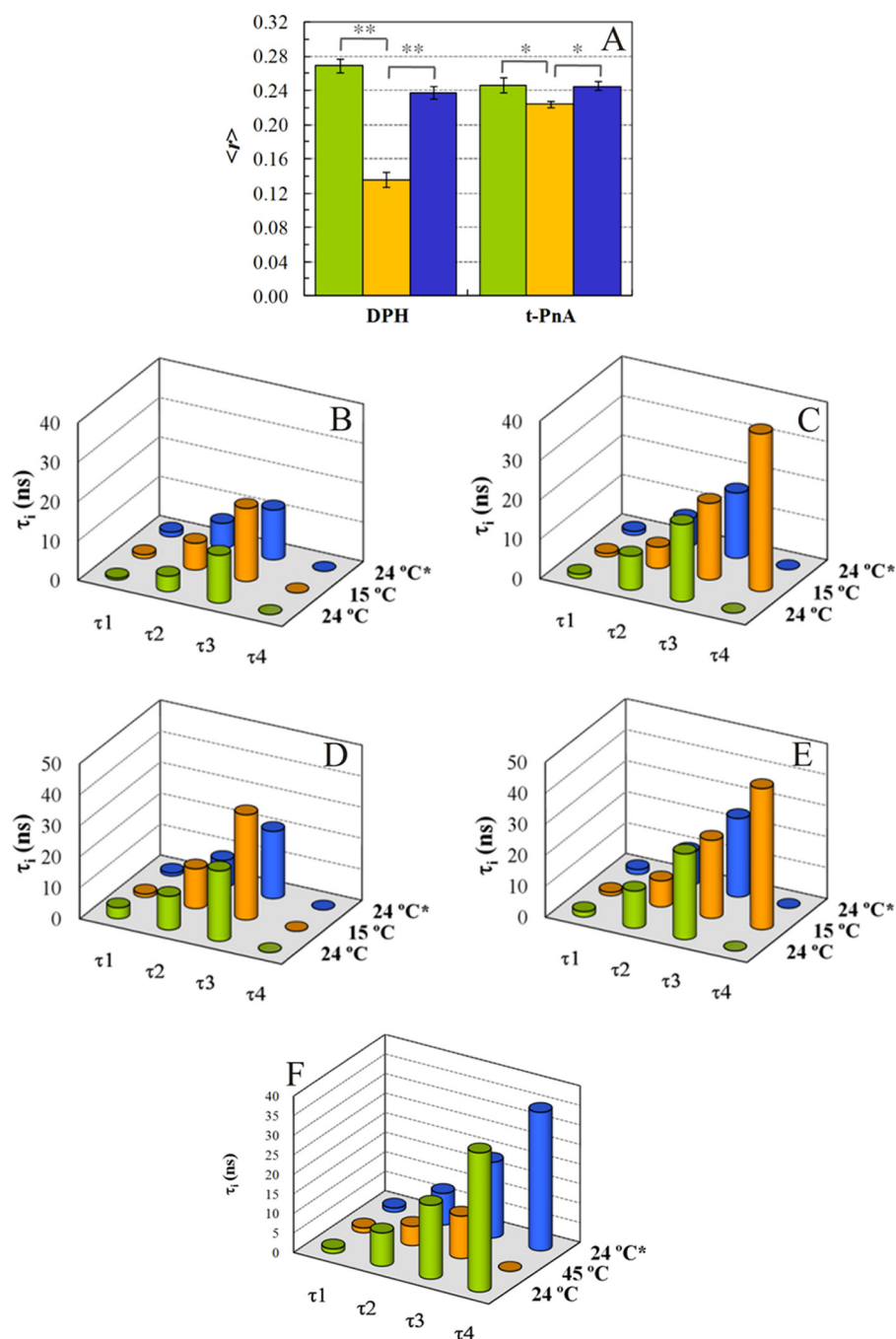


**FIGURE 3. Cer gel solubilization by Chol is reversible.** A, Cer domain formation upon Chol oxidation by Chol oxidase. DPH and *t*-PnA steady-state fluorescence anisotropy at 24 °C in POPC/Chol (60:40) mixtures containing 12 mol % PCer, before (green) and after (orange) Chol oxidase treatment. The samples were treated with 1.5 units/ml at 37 °C. In control samples, enzyme was replaced by buffer (blue). The data correspond to the average of at least three independent experiments. Comparison of means was made by Student's *t* test. Statistical significance was considered for  $p < 0.05$  (indicated by \* and by \*\* when  $p < 0.001$ ). No significant differences were found between control and untreated samples. B–F, temperature effects on PCer-rich gel domain formation and solubilization are shown. Fluorescence lifetime components of *t*-PnA, POPC/Chol (3:2) (B); POPC/Chol (3:2) with 12 mol % PCer (C); PSM/POPC/Chol (1:1:1) (D), and PSM/POPC/Chol (1:1:1) with 4 mol % PCer (E) at initial temperature (24 °C, green), after cooling (15 °C, orange), and after reheating (24 °C\*, blue). When Cer gel is formed, an extra long component ( $\tau_4$ ) is necessary to properly describe the decay. F, Cer domain solubilization and re-formation by heating-cooling. Fluorescence lifetime components of *t*-PnA are shown in PSM/POPC/Chol (1:1:1) with 8 mol % PCer at initial temperature (24 °C, green), after heating (45 °C, orange), and after recooling (24 °C\*, blue).

ing the equilibrium conditions. To determine which hypothesis is valid, the reversibility of the process has to be tested. For that purpose two different strategies were employed, enzymatic and

changed (Fig. 3A, right). These results point toward a higher solubility of Cer in Chol-rich phases than in poor ones (hypothesis 2).

temperature cycle protocols (supplemental Fig. S3). In both these protocols, Chol-containing mixtures where no PCer-rich gel is present were used as the starting point. In the enzymatic assay, samples were treated with Chol oxidase, leading to the formation of Chne. If hypothesis 1 is correct, no gel will form, and the membrane will be more disordered. Thus, both *t*-PnA and DPH fluorescence anisotropy will decrease. However, if hypothesis 2 is correct, Cer remains in the membrane, and its low solubility in POPC/Chne fluid will lead to the segregation of Cer molecules into gel domains. In this case, *t*-PnA anisotropy will not change significantly but DPH anisotropy will decrease (as in Fig. 1, D and C, respectively, going in the direction of low  $X_{\text{Chol}}$ ). The temperature cycle protocol consists of two steps as follows: (a) the samples at room temperature (~24 °C) are slowly cooled to 15 °C and the system is forced into a new thermodynamically stable state. The overall order of the system is higher, and if the formation of a PCer-rich gel phase is occurring, the *t*-PnA fluorescence decay will present an extra component longer than 35 ns (*i.e.* if hypothesis 2 is correct). If hypothesis 1 is valid, and Cer is no longer in the bilayer, no Cer-rich gel will form even at this low temperature (no extra long *t*-PnA lifetime of >35 ns); (b) the samples are slowly brought back to room temperature (24 °C), and a new set of *t*-PnA lifetimes is measured. This step is performed to examine whether the low temperature did not affect the initial equilibrium state of the system at 24 °C, ruling out any hysteresis effects.

For POPC/Chol/PCer mixtures, treatment with Chol oxidase, *i.e.* Chne formation, leads to a sharp decrease in DPH fluorescence anisotropy (Fig. 3A, left). On the other hand, *t*-PnA fluorescence anisotropy remained practically un-

The results obtained by the temperature protocol also validate hypothesis 2. In the absence of PCer, as expected, no gel is formed, and the higher lifetime component of *t*-PnA fluorescence decay is below 30 ns (Fig. 3, *B* and *D*). In the presence of PCer, and when cooling to 15 °C, an extra long lifetime component (>40 ns) is present both in raft and non-raft-forming mixtures (Fig. 3, *C* and *E*, respectively). This undoubtedly shows the formation of PCer gel domains at this temperature from mixtures that were completely in the fluid phase at 24 °C. Taken together, these results show that Cer is not displaced from the bilayer membrane and is in fact mixed with Chol and other lipids. By re-heating the samples back to 24 °C, the long lifetime component of *t*-PnA disappears (Fig. 3, *C* and *E*), showing that Cer-rich gel mixing/demixing by high amounts of Chol is a reversible process.

To test the reversibility degree of the process, a raft mixture containing 8 mol % PCer, *i.e.* one that presents PCer-rich gel domains at the starting point (Fig. 2*C*), was heated to 45 °C. In these conditions the long lifetime component of *t*-PnA is <20 ns (Fig. 3*F*). Thus, no PCer-rich gel is present at this temperature. At this temperature, there is no formation of the  $l_o$  phase (44), confirming that the dissolution of Cer gel in Chol-rich membranes is independent of  $l_o$  phase formation. The samples were then slowly cooled back to 24 °C, and the long lifetime component of *t*-PnA fluorescence decay was recovered. This result agrees well with the ones obtained for the cooling cycle, and it allows the conclusion that Cer-rich gel destruction by high amounts of Chol is reversible in both directions, regardless of whether the presence of Cer domains is the starting point or not.

## DISCUSSION

This study aimed at a better understanding of Chol-Cer interactions, an important subject in membrane biophysics. Both these two molecules present a small polar headgroup and promote phase separation when mixed with other lipids (1, 2, 12, 14), but when alone or mixed together they cannot form stable bilayers (25, 45). Cer-induced membrane alterations are highly dependent on membrane composition, particularly on Chol amounts (13, 20–23, 30).

*Solubilization of Cer Domains by Chol, Qualitative Findings*—Most studies addressing Chol-Cer interactions in model and cell membranes suggest that these molecules are competitors for the same sites in the membrane-SM-enriched fluid domains (24–29), with the implicit idea that Chol and Cer mutually segregate. In this work we observed that Chol-dependent Cer gel dissolution also occurs for non-raft forming mixtures, in which SM is absent. This result could be obtained because of the high sensitivity of the method used, which allowed for the identification of PCer-rich gel formation at high Chol and low Cer amounts, *i.e.* at physiologically relevant levels to understand the interactions at the PM. For instance, it was possible to study membrane alterations of fluid membranes with high Chol content (up to 50 mol %) induced by Cer amounts ranging from 4 to 30 mol % (Cer PM levels from resting to apoptotic cells and pathological conditions (7, 8)). Using lipid mixtures that present different phases, we clearly showed that Cer gel abolishment by Chol is independent of  $l_o$  phase formation, because the

same result was obtained in mixtures where  $l_o$  phase is not formed, as is the case of Chol mixtures with DOPC (34, 46). Solubilization of Cer gel domains occurred before the system reached the composition correspondent to a pure  $l_o$  phase. For example, 30 and 40 mol % Chol mixed with POPC abolished Cer gel for 8 and 12 mol % Cer (Fig. 1*A*), and the published phase diagram indicates that the  $l_o$  phase is 46% Chol (42). Furthermore, for the DOPC-containing system, which is more disordered than the POPC-containing one, solubilization of Cer occurs for even lower Chol mole fractions.

We also studied the mechanism by which Chol prevents Cer-rich gel domain formation. The results obtained categorically show that Cer gel is solubilized by high Chol amounts, and that it is a thermodynamically reversible process involving a mixing/demixing transition (Fig. 3, and [supplemental Fig. S2](#)).

A study of the crystal formation in POPC/Chol/Cer mixtures has shown that Chol was displaced from the bilayer when the amounts of Chol plus Cer were very high (25). This result, together with our data showing that the composition of the fluid is hardly affected by the presence of Cer (Fig. 1*C*), is evidence for the very low solubility of Chol in Cer gel (see below). Hence, Cer is indeed more soluble in Chol-rich membranes than in poor ones, both in raft and in non-raft model mixtures.

In addition to the high Chol concentrations, low Chol concentrations were also studied. These lipid mixtures resemble more the composition of intracellular membranes, such as ER and mitochondrial outer membrane. It was found that in these mixtures Cer gel formation is highly dependent on the average  $T_m$  of the phospholipids (and sphingolipids when present) mixed with Cer and Chol.

*Solubilization of Cer Domains by Chol, Quantitative Findings*—The finding that the mixing/demixing reversible transition is the mechanism by which Chol dissolves Cer gel validates the building of a phase diagram to quantitatively describe the process. Information about the number, fraction, and composition of the phase(s) that occur at a fixed temperature and pressure is given by the diagram. In Fig. 4*A*, a possible configuration of the POPC/Chol/PCer phase diagram is shown. When going from the bottom of the triangle to the top, there is an increase of Chol mole fraction, and when going from the left side of the triangle to the right, there is an increase of PCer mole fraction with a simultaneous decrease in the POPC mole fraction. The diagram presents two main regions as follows: a region where the system is in the fluid phase (*F* region in high Chol and very low Cer regimes), and a broad region where it presents fluid-gel coexistence (*F* + *G* region in low Chol and intermediate Cer regimes). Separating these two regions is the fluid-gel boundary, called the *liquidus* line. For a given mixture inside the fluid-gel region, the composition of the fluid and gel phase is given by the edges of the tie line. This is the line that contains the mixture and intersects the fluid-gel boundary (*e.g.* see *dashed line* connecting the mixtures 3 and 4 in Fig. 4*A*). Applying the lever rule to the tie line, the fraction of each phase is obtained. For instance, the fraction of gel for mixture 3 in Fig. 4*A* is equal to the distance from the left edge of the tie line to mixture 3, divided by the whole length of the tie line. The same procedure can be followed to obtain the gel fraction formed in mixture 4, and for any other mixture contained in this tie line.

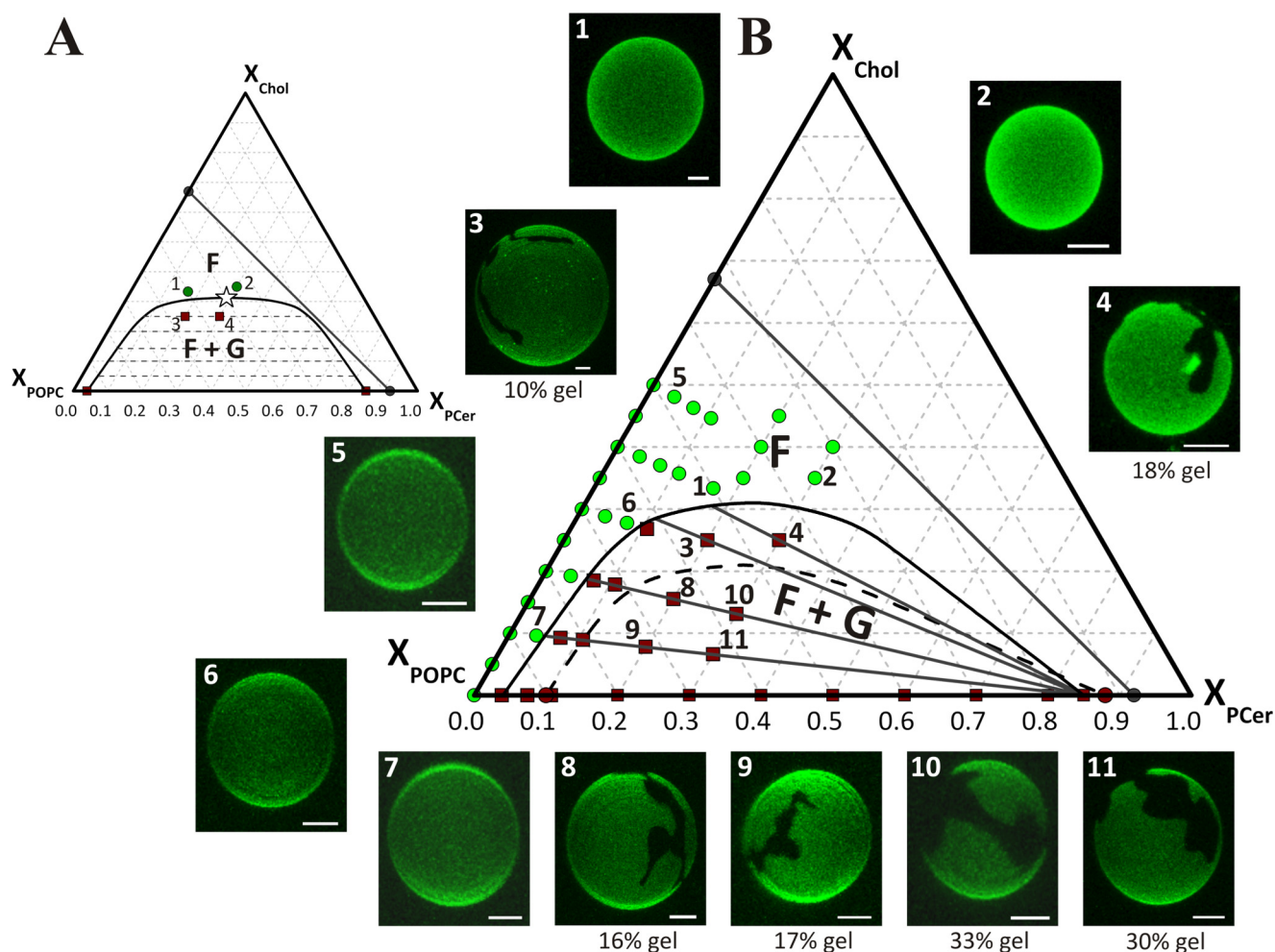


**FIGURE 4. Ternary POPC/Chol/PCer phase diagram.** *A*, schematic representation of the usual configuration of the solid-liquid phase separation region in high  $T_m$  PC/low  $T_m$  PC/Chol ternary mixtures. *B*, ternary phase diagram POPC/Chol/PCer with the experimentally determined solid-liquid phase separation region and tie lines. The symbols are experimental data points taken from Figs. 1 and 2 and supplemental Fig. S4 and from confocal microscopy images present in *B*, for which only liquid phase (green circles in the *F* region) or solid and liquid phases (red squares in the *F* + *G* region) were observed. The straight dark gray line shows the bilayer solubility limit of Chol plus Cer (15, 25). Three-dimensional projection images obtained from fluorescence confocal microscopy sections of GUV labeled with Rho-DOPE (0.2 mol %) at 24 °C for the experimental points 1–11 are shown (scale bar, 5  $\mu$ m). *A*, Chol solubility is similar in the fluid and in the gel phase. *B*, Chol solubility is much lower in the gel phase than in the fluid phase. The gel fraction formed in mixtures 3, 4, and 8–11 is indicated below each GUV image (average of more than 10 GUVs from three independent samples). It is not possible to form stable GUVs for very high Cer concentrations, and *t*-PnA fluorescence is no longer sensitive to the formation of more gel after a considerable amount of gel is present. However, it is not necessary to explore those compositions to determine the whole solid-liquid coexistence region (17, 34). In phase diagrams like the one depicted in *A*, there is a critical point (indicated as a star). However, there is no evidence for the presence of a critical point in the diagram depicted in *B*. The black dashed line indicates the gel-fluid phase coexistence region predicted for the mixture DOPC/Chol/PCer based on experimental data for that mixture and the comparison with the POPC/Chol/PCer mixture.

Using the results obtained in this study with *t*-PnA and DPH, confocal microscopy three-dimensional reconstruction of GUV (typical data in Figs. 2 and 4), and taking previous data on *t*-PnA and DPH fluorescence properties in PCer containing mixtures where PCer gel fraction was quantified (15, 17, 23), it was possible to determine quantitatively the gel/fluid coexistence region and tie lines for the ternary phase diagram POPC/PCer/Chol, and to predict qualitatively what that region would be for the DOPC/PCer/Chol system (Fig. 4).

It was reported that high levels of Chol are able to induce the mixing of two phospholipids with significant acyl-chain mismatch, abolishing their phase separation (47). In these systems, the solubility of Chol is rather similar in the gel and in the fluid phases (the diagram would look like the one depicted in Fig. 4*A*). In this case, the tie lines would be approximately horizontal (Fig. 4*A*, dashed gray lines inside the *F* + *G* region). In addition,

the gel mole fraction should be considerably higher in mixture 4 (~50% gel) than in mixture 3 (less than 30% gel). The GUV results do not support this diagram configuration. Moreover, Chol solubility in a low  $T_m$  PC and a high  $T_m$  PC is almost the same (38). This is not the case for the POPC/Chol/PCer system. The presence of Cer in the bilayer reduces the membrane solubility limit of Chol (25). This is certainly a consequence of the much lower solubility of Chol in Cer gel than that of Cer in Chol-rich fluid. In opposition to the approximately symmetric phase diagram fluid PC/gel PC/Chol (Fig. 4*A*), the fluid PC/Cer gel/Chol phase diagram is strongly asymmetric (Fig. 4*B*). The tie lines (Fig. 4*B*, gray lines in the *F* + *G* region) have a nonhorizontal direction with a negative slope, reflecting the much lower solubility of Chol in the gel than in the fluid phase. The gel mole fraction should be only slightly larger in mixture 4 than in mixture 3 (typical GUV with those composi-

tions given next to the diagram in Fig. 4B). In fact, the calculated gel fraction from the GUV for mixture 3 is 10 mol % and for mixture 4 is 20 mol %. These values are similar to the gel fraction obtained by applying the lever rule to the tie line that passes through these mixtures (12 and 18 mol %, respectively). The gel fractions formed for mixtures 8–11 (16, 17, 33, and 30 mol %, respectively) are also in good agreement with the gel fraction obtained for the nonhorizontal tie lines (17.5, 18, 30, and 31 mol %, respectively). This diagram shows how the increase in Chol solubilizes Cer gel, but it does so in a rather abrupt way. For example, following the line that contains mixtures 9, 8, and 3 (20 mol % PCer), increasing amounts of Chol (*i.e.* from the bottom of the triangle to the top), it can be seen from the tie lines that are crossed that the amount of gel is fairly constant until the fluid/gel-and-fluid boundary is approached, where it decreases sharply. The region beyond the gel-fluid coexistence is beyond the physiologically relevant Cer concentrations that are usually well below ~10 mol %, and even in pathological conditions they never exceed 20 mol % (7, 8). Comparing the coexistence region for POPC to that of DOPC, it is easily observed that the latter is shifted toward higher Cer content and lower Chol (Fig. 4B, dashed boundary *versus* gel-and-fluid boundary).

**Biological and Biophysical Implications**—The higher solubility of Cer in Chol-rich fluid phases as compared with poor ones indicates that Cer has, at least to some extent, favorable interactions with Chol molecules. The higher values obtained for *t*-PnA and DPH steady-state and time-resolved fluorescence parameters in mixtures containing PCer and high amount of Chol compared with the ones obtained in mixtures without Cer (Fig. 1) show that in mixtures containing Cer the membrane order is higher. Thus, Cer is able to increase the Chol-rich domain order even more. The reason for the higher solubility of Cer in Chol-rich membranes than in poor ones appears to be related to the ability of Chol to increase the order of fluid membranes. Cer-rich gel is formed when Chol is changed to Chne (Fig. 1B and Fig. 3A), a ketone that does not present the same ordering ability as Chol (Fig. 1B, *bottom line*, and [supplemental Fig. S1](#)). The ordered environment induced by Chol is more suitable for the insertion of Cer molecules because of the more stretched configuration of lipid acyl chains, which facilitates Cer interactions with both lipids and Chol and decreases its segregation into a Cer gel phase (Fig. 5). So, it is possible to decrease the Cer-rich gel formed in Chol-poor fluid membranes by increasing its Chol content (Figs. 1–3). This is completely opposite to what would be expected if Chol and Cer were competitors for SM-rich ordered domains. If this were the case, the increase of Chol content would result in the displacement of Cer from ordered regions to the disordered fluid, where Cer low solubility in this phase would lead to its segregation (either into a gel phase or out of the membrane), which does not happen. Recently, antibodies anti-Chol-Cer were raised, and Chol-Cer domains were identified in monolayers and in the plasma membranes of fixed cells, providing evidence for the association of these two molecules *in vitro* and *in vivo* (45). Therefore, we conclude that Chol and Cer are able to interact to a certain extent, and they do not mutually segregate when in physiological concentrations.

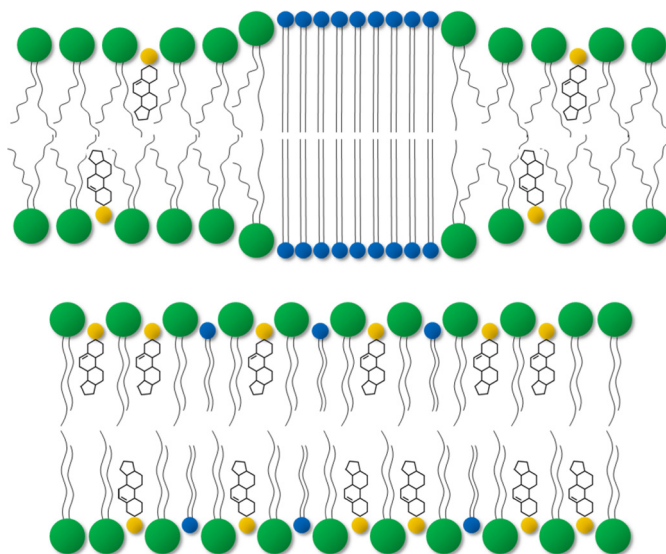


FIGURE 5. Cer is more soluble in Chol-rich membranes than in poor ones. Schematic representation of Cer lateral organization (domain formation) in Chol-poor (*top*) (Cer gel domains) and Chol-rich membranes (*bottom*) (no Cer gel domains).

It is somewhat surprising that Chol-rich membranes are able to solubilize an SL with such a high  $T_m$ , small headgroup, and low hydration as Cer. In fact, several studies indicate that Cer is able to displace Chol from ordered domains, making it more susceptible to oxidation by Chol oxidase (25), extraction by  $\beta$ -cyclodextrin (24), or high density lipoprotein (28). The higher solubility of Cer in Chol-rich membranes explains these observations. Our results show that increasing Chol content leads to a progressive decrease of Cer gel, until it is no longer present (Figs. 1 and 2 and Fig. 4B). Thus, in membranes containing Chol-poor and Chol-rich fluid phases (as in the case of raft model membranes and as proposed to occur in cell plasma membranes (48)), Cer molecules will be localized in Chol-rich domains. As a result there will be an increase of Chol chemical potential (49, 50) in these regions. This chemical potential translates the escape tendency of Chol (31). Thus, the efflux of Chol out of the plasma membrane will be facilitated, because the free energy of transfer of Chol to  $\beta$ -cyclodextrin, high density lipoprotein, or of its conversion to Chne will be lower. Therefore, Chol is more prone to oxidation by Chol oxidase and extraction by cyclodextrins or high density lipoprotein (31). In addition, the Chol potential gradient between Chol-poor and Chol-rich domains will be larger, which may also result in migration of Chol molecules to the disordered domains as suggested previously (24–29). Note that these disordered domains also include the intracellular membranes.

Furthermore, membrane phospholipid and SL content is also important. For instance, we show here that with 12 mol % PCer in DOPC/Chol, Chol in amounts higher than 30 mol % solubilizes Cer, whereas in POPC/Chol, more than 40 mol % Chol is required (Fig. 1A). In POPC/Chol with 8 mol % PCer, there is no gel for 30 mol % (Fig. 1A), whereas in raft-forming mixtures (PSM/POPC/Chol) with 33 mol % Chol, demixing of Cer does occur for 8 mol % PCer (Fig. 2, A and C). This shows that in addition to Chol/Cer ratio the “average  $T_m$ ” of the remaining lipids is equally important. When a certain threshold of Cer

concentration is reached, usually associated with pathological situations (51, 52), the formation of Cer gel domains is highly probable, both in the PM, because of the presence of SM and other high  $T_m$  lipids, and in intracellular membranes, because of their low Chol content. Note that under cell stress situations both the *de novo* synthesis of Cer and SM hydrolysis are activated, and therefore, the levels of this lipid are increased both at the ER and PM (5). In addition, the different effects of Cer on the outer and inner mitochondrial membranes (32, 33), in light of the results presented here, can be partially explained by the fact that the inner membrane is more fluid than the outer membrane (53).

Cer domain formation appears to be a requisite for Cer-induced cell apoptosis (6, 8, 19). The formation of these domains is highly dependent on Chol membrane levels. Hence, it seems that Chol/Cer ratio is one of the parameters controlling cellular fate. Interestingly, many cancer cell lines present high concentrations of Chol in the plasma membrane (54, 55). When Chol levels are diminished either by inhibitors of Chol synthesis or by extraction with cyclodextrin, the cells undergo apoptosis in a Chol plasma membrane level-dependent manner. Cells with lower plasma membrane Chol are more susceptible to apoptosis than the respective ones with normal membrane Chol content (54, 55). A regulatory function of a Chol/Cer plasma membrane ratio in Cer-mediated apoptosis is also suggested by strategies that tumors develop to reduce Cer levels. Some types of tumors reduce the expression of acid sphingomyelinase, which is the main enzyme that produces Cer in the plasma membrane, or increase the expression of glucosyltransferases that catalyze Cer conversion to glucosyl- or lactosyl-Cer (56–60). In addition, it was shown that membranes of multidrug-resistant cancer cell lines present elevated levels of Chol and glucosyl-Cer regarding its nonresistant counterparts (57, 61). Targeting Chol and Cer metabolism to restore or even increase Cer-induced plasma membrane alterations may provide an opportunity to eliminate tumors by induction of apoptosis.

### REFERENCES

- Ohvo-Rekilä, H., Ramstedt, B., Leppimäki, P., and Slotte, J. P. (2002) *Prog. Lipid Res.* **41**, 66–97
- Mouritsen, O. G., and Zuckermann, M. J. (2004) *Lipids* **39**, 1101–1113
- London, E., and Brown, D. A. (2000) *Biochim. Biophys. Acta* **1508**, 182–195
- Stöckl, M., Plazzo, A. P., Korte, T., and Herrmann, A. (2008) *J. Biol. Chem.* **283**, 30828–30837
- Hannun, Y. A., and Obeid, L. M. (2008) *Nat. Rev. Mol. Cell Biol.* **9**, 139–150
- Grassmé, H., Riehle, A., Wilker, B., and Gulbins, E. (2005) *J. Biol. Chem.* **280**, 26256–26262
- Hannun, Y. A. (1996) *Science* **274**, 1855–1859
- Cremesti, A. E., Goni, F. M., and Kolesnick, R. (2002) *FEBS Lett.* **531**, 47–53
- van Blitterswijk, W. J., van der Luit, A. H., Veldman, R. J., Verheij, M., and Borst, J. (2003) *Biochem. J.* **369**, 199–211
- Taha, T. A., Mullen, T. D., and Obeid, L. M. (2006) *Biochim. Biophys. Acta* **1758**, 2027–2036
- Shah, J., Atienza, J. M., Duclos, R. I., Jr., Rawlings, A. V., Dong, Z., and Shipley, G. G. (1995) *J. Lipid Res.* **36**, 1936–1944
- Holopainen, J. M., Lehtonen, J. Y., and Kinnunen, P. K. J. (1997) *Chem. Phys. Lipids* **88**, 1–13
- Massey, J. B. (2001) *Biochim. Biophys. Acta* **1510**, 167–184
- Hsueh, Y. W., Giles, R., Kitson, N., and Thewalt, J. (2002) *Biophys. J.* **82**, 3089–3095
- Silva, L., de Almeida, R. F., Fedorov, A., Matos, A. P., and Prieto, M. (2006) *Mol. Membr. Biol.* **23**, 137–148
- Sot, J., Bagatolli, L. A., Goñi, F. M., and Alonso, A. (2006) *Biophys. J.* **90**, 903–914
- Castro, B. M., de Almeida, R. F., Silva, L. C., Fedorov, A., and Prieto, M. (2007) *Biophys. J.* **93**, 1639–1650
- Kolesnick, R. N., Goñi, F. M., and Alonso, A. (2000) *J. Cell. Physiol.* **184**, 285–300
- Bollinger, C. R., Teichgräber, V., and Gulbins, E. (2005) *Biochim. Biophys. Acta* **1746**, 284–294
- Chiantia, S., Kahya, N., Ries, J., and Schwille, P. (2006) *Biophys. J.* **90**, 4500–4508
- Fidorra, M., Duelund, L., Leidy, C., Simonsen, A. C., and Bagatolli, L. A. (2006) *Biophys. J.* **90**, 4437–4451
- Johnston, I., and Johnston, L. J. (2006) *Langmuir* **22**, 11284–11289
- Silva, L. C., de Almeida, R. F., Castro, B. M., Fedorov, A., and Prieto, M. (2007) *Biophys. J.* **92**, 502–516
- Alanko, S. M., Halling, K. K., Maunula, S., Slotte, J. P., and Ramstedt, B. (2005) *Biochim. Biophys. Acta* **1715**, 111–121
- Ali, M. R., Cheng, K. H., and Huang, J. (2006) *Biochemistry* **45**, 12629–12638
- Björkqvist, Y. J., Nyholm, T. K., Slotte, J. P., and Ramstedt, B. (2005) *Biophys. J.* **88**, 4054–4063
- Megha and London, E. (2004) *J. Biol. Chem.* **279**, 9997–10004
- Ito, J., Nagayasu, Y., and Yokoyama, S. (2000) *J. Lipid Res.* **41**, 894–904
- Yu, C., Alterman, M., and Dobrowsky, R. T. (2005) *J. Lipid Res.* **46**, 1678–1691
- Silva, L. C., Futerman, A. H., and Prieto, M. (2009) *Biophys. J.* **96**, 3210–3222
- Lange, Y., and Steck, T. L. (2008) *Prog. Lipid Res.* **47**, 319–332
- Siskind, L. J., Kolesnick, R. N., and Colombini, M. (2006) *Mitochondrion* **6**, 118–125
- Novgorodov, S. A., Guduz, T. I., and Obeid, L. M. (2008) *J. Biol. Chem.* **283**, 24707–24717
- de Almeida, R. F., Borst, J., Fedorov, A., Prieto, M., and Visser, A. J. (2007) *Biophys. J.* **93**, 539–553
- de Almeida, R. F., Loura, L. M., Fedorov, A., and Prieto, M. (2002) *Biophys. J.* **82**, 823–834
- Pinto, S. N., Silva, L. C., de Almeida, R. F., and Prieto, M. (2008) *Biophys. J.* **95**, 2867–2879
- Veatch, S. L., and Keller, S. L. (2005) *Phys. Rev. Lett.* **94**, 148101
- Thewalt, J. L., and Bloom, M. (1992) *Biophys. J.* **63**, 1176–1181
- de Almeida, R. F., Loura, L. M., Fedorov, A., and Prieto, M. (2005) *J. Mol. Biol.* **346**, 1109–1120
- Davis, J. H., Clair, J. J., and Juhasz, J. (2009) *Biophys. J.* **96**, 521–539
- de Almeida, R. F., Loura, L. M., and Prieto, M. (2009) *Chem. Phys. Lipids* **157**, 61–77
- de Almeida, R. F., Fedorov, A., and Prieto, M. (2003) *Biophys. J.* **85**, 2406–2416
- Xu, X., and London, E. (2000) *Biochemistry* **39**, 843–849
- Bunge, A., Müller, P., Stöckl, M., Herrmann, A., and Huster, D. (2008) *Biophys. J.* **94**, 2680–2690
- Scheffer, L., Futerman, A. H., and Addadi, L. (2007) *ChemBioChem* **8**, 2286–2294
- Schroeder, R., London, E., and Brown, D. (1994) *Proc. Natl. Acad. Sci. U.S.A.* **91**, 12130–12134
- Silvius, J. R., del Giudice, D., and Lafleur, M. (1996) *Biochemistry* **35**, 15198–15208
- Simons, K., and Toomre, D. (2000) *Nat. Rev. Mol. Cell Biol.* **1**, 31–39
- Radhakrishnan, A., and McConnell, H. M. (2000) *Biochemistry* **39**, 8119–8124
- Radhakrishnan, A., Anderson, T. G., and McConnell, H. M. (2000) *Proc. Natl. Acad. Sci. U.S.A.* **97**, 12422–12427
- Birbes, H., Luberto, C., Hsu, Y. T., El Bawab, S., Hannun, Y. A., and Obeid, L. M. (2005) *Biochem. J.* **386**, 445–451
- García-Ruiz, C., Colell, A., Marí, M., Morales, A., and Fernández-Checa, J. C. (1997) *J. Biol. Chem.* **272**, 11369–11377
- Hackenbrock, C. R., Höchli, M., and Chau, R. M. (1976) *Biochim. Biophys.*

- Acta* **455**, 466–484
54. Freeman, M. R., and Solomon, K. R. (2004) *J. Cell. Biochem.* **91**, 54–69
55. Li, Y. C., Park, M. J., Ye, S. K., Kim, C. W., and Kim, Y. N. (2006) *Am. J. Pathol.* **168**, 1107–1118; quiz 1404–1405
56. Gouazé, V., Yu, J. Y., Bleicher, R. J., Han, T. Y., Liu, Y. Y., Wang, H., Gottesman, M. M., Bitterman, A., Giuliano, A. E., and Cabot, M. C. (2004) *Mol. Cancer Ther.* **3**, 633–639
57. Lavie, Y., Cao, H., Bursten, S. L., Giuliano, A. E., and Cabot, M. C. (1996) *J. Biol. Chem.* **271**, 19530–19536
58. Liu, Y. Y., Yu, J. Y., Yin, D., Patwardhan, G. A., Gupta, V., Hirabayashi, Y., Holleran, W. M., Giuliano, A. E., Jazwinski, S. M., Gouaze-Andersson, V., Consoli, D. P., and Cabot, M. C. (2008) *FASEB J.* **22**, 2541–2551
59. Senchenkov, A., Litvak, D. A., and Cabot, M. C. (2001) *J. Natl. Cancer Inst.* **93**, 347–357
60. Sietsma, H., Veldman, R. J., and Kok, J. W. (2001) *J. Membr. Biol.* **181**, 153–162
61. Lavie, Y., Fiucci, G., Czarny, M., and Liscovitch, M. (1999) *Lipids* **34**, Suppl. S57–S63